Low-Cognitive-Load Navigation System for the Visually Impaired Using Head Rotation

Shinya Kajikawa [1,*] and Satoshi Koharada [2]

[1] Department of Mechanical Engineering and Intelligent Systems, Faculty of Engineering, Tohoku Gakuin University, Sendai, Japan

[2] Hamamatsu Plant, MinebeaMitsumi Inc., Fukuroi, Japan

Email: kajikawa@mail.tohoku-gakuin.ac.jp (Sh.K.); skoharada@minebeamitsumi.com (Sa.K.)

*Corresponding author

***Abstract*—Numerous walking navigation systems have been developed that convert spatial information into auditory or tactile stimuli for user perception. However, these systems often burden users with the cognitive task of interpreting their environment based on limited sensory input. We propose a novel navigation system that reduces the cognitive load by inducing trunk motion through head direction control. This method focuses on the characteristic of the trunk following the head yaw motion during walking. In this paper, we have fabricated a prototype navigation system consisting of both a head rotation control unit and a sensing unit with a depth camera. Using this system, we investigated the feasibility of the proposed method in actual navigation. First, we confirmed through several experiments that the walking direction changes according to the forced head direction control. This result supports the feasibility of the proposed method. Then, we developed a head control scheme that combines two head control modes to improve the accuracy and stabilization of the direction change. One is a forced rotation mode toward the target direction, and the other is a free rotation mode to align the direction of the head and the trunk. Finally, to verify the feasibility of two-mode control in a real environment, a navigation experiment was conducted to avoid a single obstacle. This experiment confirmed that reliable avoidance guidance was achieved.**

***Keywords*—walking navigation, low cognitive load, visually impaired person, hands-free, head rotation control, obstacle avoidance**

I. Introduction

In 2020, an estimated 338 million people worldwide will be visually impaired, of which 43 million will be totally blind and 295 million will have moderate to severe visual impairment [1]. Social participation of the visually impaired is essential for their independence and well-being, and mobility assistance plays an important role in facilitating this social participation.

While guide dogs and white canes are common mobility aids for the visually impaired, they present significant accessibility challenges. Guide dogs provide invaluable assistance. However, their training is extensive and costly, resulting in a limited supply. White canes, on the other hand, are more readily available, but require the acquisition of operating skills for effective environmental perception. These limitations hinder their widespread adoption as accessible mobility solutions for the visually impaired community.

In response to these limitations, a number of Electronic Travel Aids (ETAs) with environmental sensing capabilities have been developed in recent years. These devices use technologies such as an infrared sensor, an ultrasonic sensor, and a depth camera to detect obstacles and safe walking paths. They also convey the acquired spatial information to the user through auditory or haptic feedback [2–14].

Auditory feedback is often a practical limitation in assistive walking applications because the visually impaired already rely on sound for spatial perception [15]. Exposure to auditory feedback can interfere with and reduce the user's auditory abilities. As a result, posture and balance may be disrupted, which could have a significant impact on social interactions.

Some wearable ETAs use multiple vibration stimulus locations to convey walking commands through the combinations of these stimuli [12–14]. However, sequential stimulation results in delays in information delivery. In addition, the commands given are simple and cannot provide the fine directional adjustments needed for precise navigation. Instead of vibration stimulation, a device that applies shear deformation to the skin using cuffs worn on the upper arm has also been proposed [11]. It potentially causes faster user response, but also has limitations in providing detailed directional guidance. All these approaches provide limited information, leaving important gait planning to the user.

There is a strong demand for ETAs that can actively guide users in a safe direction. GuideCane [16], Guide-Dog and Cabot are examples of such systems. GuideCane is a white cane equipped with an ultrasonic sensor and a steering mechanism [17, 18]. By controlling the steering, it guides the user to avoid obstacles. Guide-Dog and CaBot are mobile robotic systems modeled after guide dogs, and the user is guided by walking through a rope or handle held

Manuscript received April 25, 2024; revised July 25, 2024; accepted August 6, 2024; published January 9, 2025.

in the hand. These systems use the torque or traction force applied to the user's hand to actively guide the user's gait. A hands-free device has also been developed that directly controls the user's trunk orientation to avoid obstacles [19]. This device guides the user based on depth camera information using two steering wheels attached to the tips of links connected to the user's left and right hips. Since trunk orientation is directly controlled, the user is guided subconsciously, but it is bulky. These systems provide intuitive guidance and are very easy to use. However, they have the disadvantage of restricting hand movement and being bulky.

As discussed above, existing ETAs that provide sensory feedback suffer from two major limitations. First, users must rely on limited feedback information to perceive their environment. Processing this information can be cognitively demanding. Second, users themselves must adjust their walking based on this limited information. This can be difficult and error prone. Alternatively, systems that actively guide users can limit their physical freedom by requiring them to hold bulky devices or interact with the system. This can ultimately limit their overall mobility.

This paper proposes a novel walking guidance method that utilizes the unconscious trunk response that follows head movements. This method is based on the characteristic that humans change their walking direction by rotating their trunk in the same direction as their head. Users can obtain walking direction information directly by having their head direction controlled by a head-mounted device. This method is very user-friendly because it does not require any device operation or complex information processing.

To verify the potential of the proposed method, a prototype consisting of a depth camera and a head rotation control device was fabricated and three experiments were conducted using it. The first experiment confirmed that walking direction can be effectively adjusted based on head rotation control. The second experiment validated the method of combining two control modes to stabilize walking direction after the trunk rotation. Finally, a real-world walking guidance experiment was conducted, and successful obstacle avoidance was demonstrated. These results indicate that the walking guidance method based on head rotation has the potential to be a valuable tool for visually impaired people.

II. Related Works

A. Head Rotation in Walking

Turning is a critical component of adaptive locomotion, and numerous gait analyses have been conducted to elucidate its control mechanisms or to predict its trajectory [20]. These studies have examined gait patterns during curved paths and heading changes toward presented targets, analyzing gaze, head, and trunk movements. Results consistently show that gaze, head, and trunk orientations change sequentially toward the target direction, culminating in walking toward the target. The timing of these directional changes has also been studied in detail [21–23].

Interestingly, it has been confirmed that head yaw precedes trunk yaw during turning, even when visual information is blocked [24]. Furthermore, unexpected head rotations during walking can significantly alter the walking trajectory [25, 26], highlighting the critical role of the head orientation in locomotion.

Even in the field of neuroscience, the head is recognized as a site that predicts the direction of movement and provides a stable reference system for coordinating the movements of the rest of the body [27], supporting the above observations. These results suggest that it is possible to navigate walking by externally controlling the orientation of the head.

B. Guidance without Cognitive Load

A walking guidance system that reduces the burden of cognitive processing of spatial information has been proposed. One that manipulates walking direction by Functional Electrical Stimulation (FES) to the thigh has been proposed [28]. Galvanic Vestibular Stimulation (GVS), a technique that applies electrical currents near the ears to alter balance sensation, was used to control walking direction [29]. However, these methods using electrical stimulation have issues with certainty.

Attempts have also been made to walking navigation using a pseudo-force perception called the hanger reflex. The hanger reflex is a phenomenon in which shear deformation of the skin creates the illusion of force and involuntary rotation of body parts, which can occur in various parts of the body. Several experiments have been conducted to control walking direction using reflexes in the head, waist, and ankle, but the effects have been reported to be limited, with the exception of the waist reflex [30].

The magnitude of this reflex response varies between individuals, making it difficult to guide the subject in the expected direction. Reliable navigation requires a system that can direct the user accurately in the target direction.

III. Navigation System Using Head Rotation

A. System Overview

Fig. 1 shows the configuration of the proposed system. The system consists of a sensing environment unit and a head rotation control unit. In the sensing environment unit, a depth camera (Oak-D OpenCV Depth AI Camera, Luxonis), mounted on the chest for detecting obstacles and exploring passable areas, was used.

Based on this information, the head rotation control unit directed the user's head towards the passable area. Two microcontrollers, Raspberry Pi 3 model B+ and Arduino Due, were used to control the depth camera and the head rotation control device, respectively.

These microcontrollers communicated with each other via serial communication.

B. Head Rotation Control Device

Fig. 2 shows the user-worn head rotation device and its control unit. The device was attached to the user's back with a rigid link. The head rotation angle, θ, is defined in a coordinate system based on the coronal and sagittal planes. The head rotation control unit used a DC geared motor with an encoder (FIT0493, 12V, DFROBOT) and a rack and pinion system to either gently guide the user's head in the desired direction (Controlled Rotation Mode) or follow the user's intended head motion (Free Rotation Mode).

The motor has a stall torque of 12 kg-cm and weighs only 98 g. The rack and pinion system (DR1-200 and SSDR1-30, module = 1.0, KHK Gears) was attached to the curved frame made of acrylic resin mounted around the head and weighed about 60 g. The total weight of the head rotation control device was about 500 g. Most of the weight was due to the two stainless steel plates that supported the motor and the rack and pinion system. Because it was supported by the back via links, head motion was not significantly impeded. The motor driver (Sabertooth Dual 10 A, Dimension Engineering) and battery (Li-ion Rechargeable 12 V) were housed in an acrylic plastic storage case carried on the back.

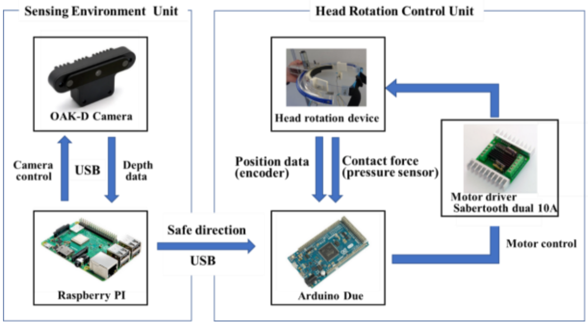

Fig. 1. Configuration of the proposed navigation system.

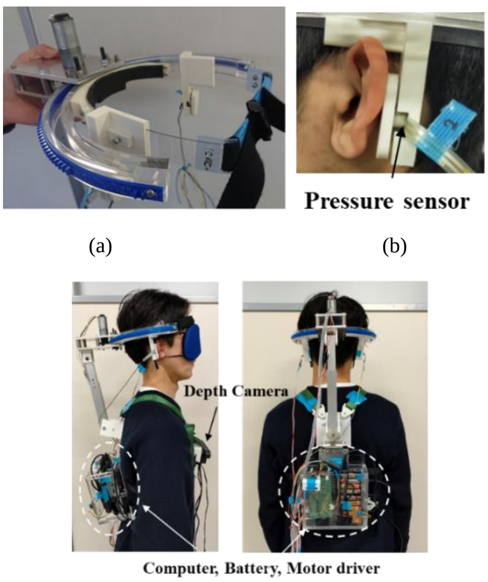

(a) (b)

(c)

Fig. 2. Prototype of a walking navigation system. (a) The head rotation device is attached to the back by a pin-coupled link. Therefore, the forward and backward movement of the head is not restricted. (b) The ear pads must be adjusted to maintain constant contact with the back of the ear to properly sense the contact force. (c) Whole system: the backpack contains two microcontrollers, a motor driver, and batteries.

C. *Head Rotation Mode*

In Controlled Rotation Mode, which is activated by the detection of obstacles and safe passages, the system sets the target head angle, θ_d, and the duration of the head rotation, t_f to generate the head motion. The head position is controlled according to the minimum jerk model [31]. The minimum jerk model generates a motion that minimizes acceleration changes, which is expected to be gentler for the user.

In Free Rotation Mode (the default mode), the head rotation control device continuously monitors pressure sensors (FSR402, Interlink Electronics) positioned behind each ear (Fig. 2(b)). It detects the user's intention to rotate the head to the right or left based on the difference in pressure values. Based on this intention, the device adjusts its motion to follow the user's desired head movement. The rotational velocity is controlled in proportion to the difference in the pressure values.

In each mode, the control system used the walkable direction, θ_d, or the difference in contact pressure values to calculate the desired head angle, $\theta(t)$, or angular velocity, $\dot{\theta}(t)$, at each sampling step, t, respectively.

These processes are described as Eqs. (1) and (2).

Controlled Rotation Mode (Minimum Jerk Model)

$$\theta(t) = \theta_d\left[6\left(\frac{t}{t_f}\right)^5 - 15\left(\frac{t}{t_f}\right)^4 + 10\left(\frac{t}{t_f}\right)^3\right] \quad (1)$$

Free Rotation Mode

$$\dot{\theta}(t) = \begin{cases} K(f_l(t) - f_r(t)) = K\Delta f(t) & (|\Delta f(t)| > f_{th}) \\ 0 & (|\Delta f(t)| \le f_{th}) \end{cases} \quad (2)$$

where, f_l, f_r, and Δf indicate the contact pressure values with the left and right ear and the difference between their forces, respectively. f_{th} and K are the threshold value and the gain parameters, respectively. The threshold value is used to reduce the influence of noise on the following movement. The gain parameter adjusts the sensitivity of the pressure sensors.

D. *Sensing Walking Area for Safe Navigation*

For safe navigation, the depth camera must detect obstacles within the walking area to determine a collision-free route. In addition, the navigation should be updated in real time. This requires a simple yet effective approach. To ensure safe navigation, the depth camera was mounted on the chest at 1.2 m above the ground. We confirmed that this vantage point allowed reliable observation of the ground surface beyond 4 m ahead, even when the upper body moved up and down during walking. This 4 m range was considered sufficient for safe maneuvering to avoid obstacles.

To shorten processing time, we prioritized the area closest to the ground for search, assuming that obstacles were more likely to be located there. This was achieved by defining nine sequential Regions of Interests (ROIs), each measuring 160×128 pixels, at the bottom of the depth image. Each ROI corresponded to a real-world width of approximately 0.55 m at a distance of 4.0 m ahead. The presence of obstacles within a region was inferred when the average depth value fell below 3.0 m, while the absence of obstacles was inferred when it exceeded 3.0 m.

If adjacent obstacle-free regions were found, they were merged to increase the traversable area. Finally, the largest identified traversable region was selected as the passage region and its center was set as the target position. If the system could combine two or more consecutive ROIs, this indicated a sufficient space for safe passage. Fig. 3 shows the expected result of running our algorithm in an environment with two obstacles. Here, the combined region of ROIs #7, #8, and #9 is identified as the traversable area, representing the largest available space.

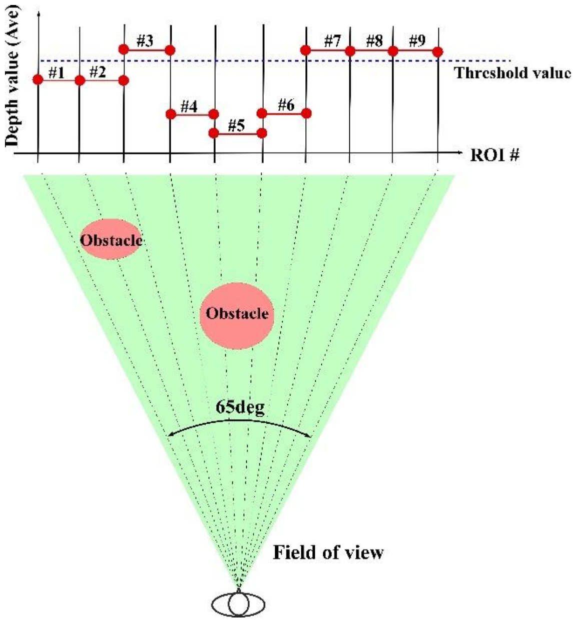

Fig. 3. Example of depth information obtained using our algorithm. The horizontal viewing angle of 65 degrees is divided into 9 sections and each ROI is created. The red line in the upper graph shows the average distance value for each ROI.

Fig. 4 shows an actual result of the traversable area detection using our algorithm. This result recommended the center of ROI #4 as the target direction for navigation.

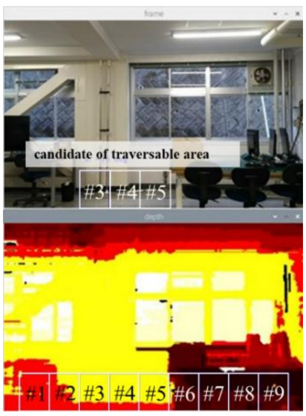

Fig. 4. Actual result of traversable area detection. In this case, a series of ROIs from #3 to #5 have been selected as traversable regions. The center of these ROIs is calculated as the actual target direction.

The target direction was calculated from the direction angles of individual Regions of Interests (ROIs). These ROIs were formed by dividing an approximately 65 deg field of view into nine equal sections, yielding an individual ROI angle of approximately 15.6 deg.

Consequently, the direction angles of the centers of ROIs #1 through #9, $\theta_1 - \theta_9$, were −28.8, −21.6, −14.4, −7.2, 0.0, 7.2, 14.4, 21.6, 28.8 deg, respectively (−: left direction, +: right direction).

In case of Fig. 4, the passable direction, θ_{pass} , is given as follows,

$$\theta_{pass} = \frac{\theta_3 + \theta_4 + \theta_5}{3} = \frac{-14.1 - 7.2 - 0.0}{3} = -7.2 \text{ deg.}$$

To ensure the trunk faced the passable direction θ_{pass} while walking, the head rotation device rotated the user's head toward θ_d with $\theta_d = \theta_{pass}$. This operation was based on Eq. (1).

IV. Walking Trajectories Following Head Rotaion

A. Procedures

To investigate how walking trajectory changes in response to head orientation, we conducted two experiments, Experiments 1 and 2.

Experiment 1: Subjects were blindfolded and walked straight ahead for 3 m while wearing the head rotation control device. Their heads were then rotated either 30 or 60 deg to the left or right for either 1 or 2 s, following the procedure described in Eq. (1). Once the head reached the target position, it was fixed. Subjects were instructed to continue walking in the direction their head was pointing.

Experiment 2: Target head positions of 30 and 45 deg were set for this experiment. As in Experiment 1, subjects walked blindfolded for 3 m. After reaching the target head position, the head was unlocked, allowing for free movement. This free movement was achieved using the strategy described in Eq. (2), with a threshold value, f_{th}, of 1.6 N.

B. Data Collection

In both experiments, the subject's position, trunk orientation, and head angle were measured. The subject's position was measured using a motion capture system (Kinema Tracer, sampling rate 120 Hz, KISSEI COMTEC CO., LTD.) that tracked two markers attached to the left and right shoulders.

The position of the subject was defined as the midpoint of the two markers. The trunk orientation, $\emptyset$, was calculated as the change of the sagittal axis in the measurement coordinate system (X-Y). The head angle, θ , was calculated using the rotation angle of the motor of the head rotation control device. This angle was defined in the trunk coordinate system (x_{trunk}-y_{trunk}), which consists of the coronal and sagittal planes. These definitions are shown in Fig. 5.

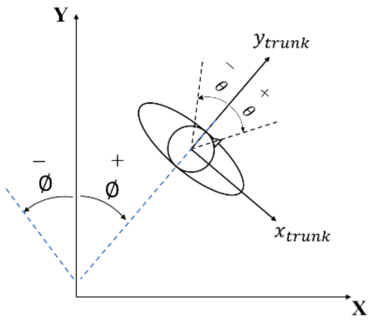

Fig. 5. Definition of head angle, θ, and trunk angle, $\emptyset$.

C. Subjects

Three subjects (Sub.A, B, C), healthy sighted males in their twenties, participated in these experiments. They performed each experiment twice. The contents and purpose of these experiments were explained to the participants, and their written consent was obtained. The study was also approved by the ethics committee of Tohoku Gakuin University.

D. Results

Fig. 6 shows typical results from Experiments 1 and 2. In these figures, the circles and the crosses indicate the start and the end positions of the head rotation, respectively. Fig.6(a) shows that the subject drew a curved path.

In Experiment 1, the head was fixed at the final position of its rotation, so the directional misalignment between the head and the trunk remained. As the subject continued to adjust the orientation of the trunk to reduce this misalignment, the trajectory became curvilinear. As the target angle of head rotation increases, the curvature of the walking trajectory also tends to increase. This is due to the increasing misalignment between the head and trunk directions.

In contrast, Fig.6(b) shows that the subject was able to walk straight in the direction where the head eventually pointed. The subjects were free to move their heads after the initial rotation. Reversing the head rotation during this period may have quickly reduced the displacement with the trunk direction, resulting in a straight walking path that roughly followed the target direction of the head.

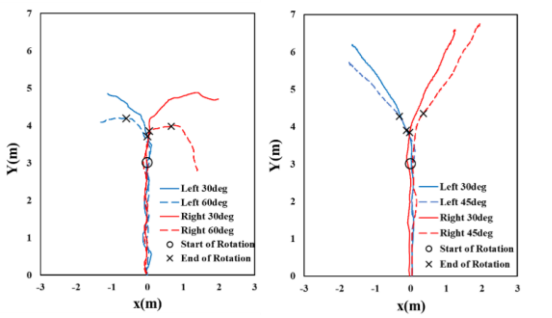

(a) (b)

Fig. 6. Walking trajectories observed in Experiments 1 and 2. (a) Experiment 1 (Sub.A): The tendency to continue rotating is confirmed by the unresolved misalignment between the head and trunk directions. (b) Experiment 2 (Sub.B): After completing the head rotation, a straight trajectory is observed.

This is confirmed by the time histories of the head and trunk angles shown in Fig. 7. After the head rotation is complete, the head returns slightly in front of the trunk, and the trunk's rate of rotation decreases at the same time. These coordinated movements align the head and trunk in approximately the same direction, which stabilizes the gait, but also creates a slight deviation from the target direction, which is a drawback.

From the results of Experiment 2, we analyzed the relationship between the target angle of head rotation and the walking direction after the head-trunk misalignment was eliminated. The results are shown in Fig. 8. From this figure, it can be confirmed that the amount of change in walking direction differed significantly depending on the target head rotation angle (T-test, $p<0.05$). We also found that the change in walking direction was smaller than the target head angle, and that left turns tended to be larger than right turns. There are two main reasons for this phenomenon.

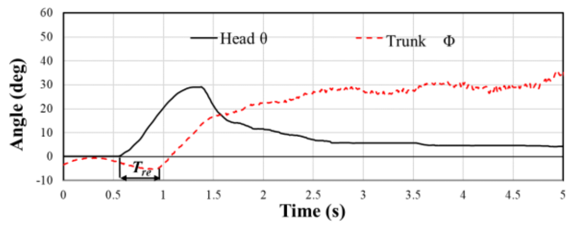

(a) Experiment 2 (the target head direction : right 30deg)

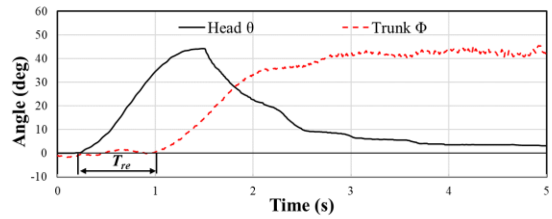

(b) Experiment 2 (the target head direction : right 45deg)

Fig. 7. Temporal changes in head and trunk orientation. After completion of the head rotation to the target angle, a free-motion segment was introduced. During this free-motion segment, the inversion of head motion began, and the deceleration of trunk motion in response to this head inversion maintained walking direction.

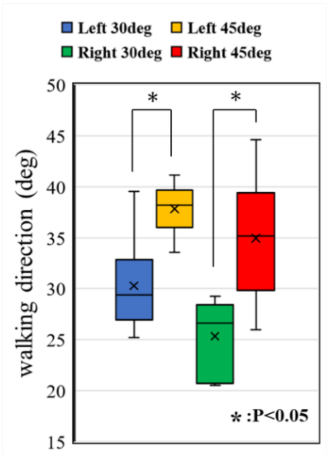

Fig. 8. Walking direction for each head rotation. It can be seen that the walking direction changes with the head rotation angle. However, it is smaller than the head rotation angle.

First, the head moves to restore the misalignment with the trunk, as mentioned above. Second, the foot, which kicks forward at the beginning of the head movement is thought to influence the results.

In walking, when the head turns, the trunk turns first to follow the head, and then the whole body turns around the standing leg. When the head rotates to face the opposite side of the swinging leg, the pivoting motion of the trunk allows the landing position of the swinging leg to be closer to the direction the head is facing. This allows for smoother and larger changes in walking direction. It can be inferred that counterclockwise head rotation often satisfies this condition.

Next, the reaction time of the trunk to the head rotation was investigated. The reaction time, T_{re} ,was defined as the time from the onset of head rotation to the onset of trunk rotation in the same direction (Fig. 7). Fig. 9 summarizes the reaction time of each subject in Experiment 1 and 2. Analysis of these results shows that trunk movements begin within approximately 700–1200 ms. The reason for the variation is, as mentioned above, whether the head was rotating toward the swinging side.

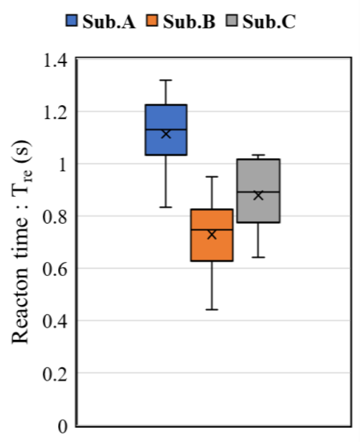

Fig. 9. Reaction time of the trunk.

V. Navigation to Avoid Obstacle

In Section IV, we confirmed that the walking direction changes depending on the head direction. However, in everyday life, there are many situations where the walking direction needs to be continuously changed, such as walking through a corridor with many turns or avoiding obstacles. Therefore, in this section, we assume the simplest task of avoiding a single obstacle and confirm whether it is possible to achieve stable walking navigation by consecutively controlling the head direction using the method shown in Experiment 2.

A. Head Orientation for Collision Avoidance

As noted in Section IV, it is necessary to allow free head movement for gait stabilization, which may result in a slight deviation from the initial target direction. Preliminary experiments have also confirmed that a small head rotation may not induce sufficient trunk motion. To address this, we propose to set a coarser target direction for the head, θ_d, based on the direction of free area, θ_{pass}, provided by the depth camera, as follows:

$$
\begin{aligned}
&if\ \ \theta_{pass} = 0\ deg. && then\ \ \theta_d = \ \ 0.0\ deg.\\
&if\ \ 0 < \theta_{pass} \leq 22.0\ deg. && then\ \ \theta_d = 30.0\ deg.\\
&if\ \theta_{pass} > 22.0\ deg. && then\ \ \theta_d = 45.0\ deg.
\end{aligned}
$$

We set the target angles larger than the value suggested by the depth camera, because the actual walking direction tended to be smaller than the target angle (Fig. 8). The head position was controlled to reach the chosen target angles of 30 deg or 45deg, using Eq. (1). The control duration was set to 1.0 s for the 30 deg target and 1.5 s for the 45 deg target.

B. Flow of Navigation for Obstacle Avoidance

The following describes the procedure for the walking navigation:

1. The subject starts walking straight ahead.
2. If the depth camera detects an obstacle, the walkable area is searched.
3. The subject's head orientation is controlled based on the direction of the detected walkable area.
4. When the head orientation reaches the target angle, a 1.0 s free head movement period is provided.
5. During this period, the subject eliminates the torsion between the head and trunk, and continues walking in the direction changed by the head movement.
6. The depth camera starts to detect obstacles again.
7. Step 2) −6) is repeated.

These operations are summarized in Fig. 10.

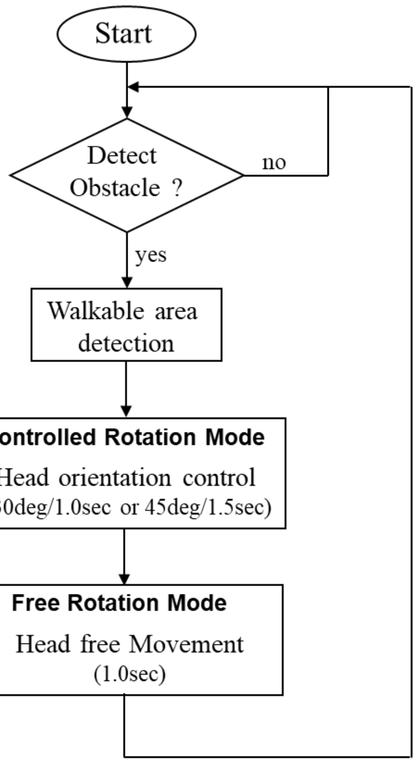

Fig. 10. Flow of guidance for obstacle avoidance.

C. Procedures

The experimental environment is shown in Fig. 11. The experiment was conducted in an indoor environment with a width of 5.0 m and a depth of 8.0 m. An obstacle with a height of 0.75 m and a depth of 0.7 m was placed in the walking area. Two locations, Case 1 and Case 2, were prepared for the installation of the obstacle, as shown in Fig. 11.

In Case 1, the obstacle was placed 4.0 m forward and 0.7 m to the right of the start position. In Case 2, the obstacle was placed 4.0 m forward to completely block the walking path. The obstacle protruded 0.4 m to the left of the walking path. Subjects were instructed to start walking straight and to continue walking in the direction of their head orientation as dictated by the device.

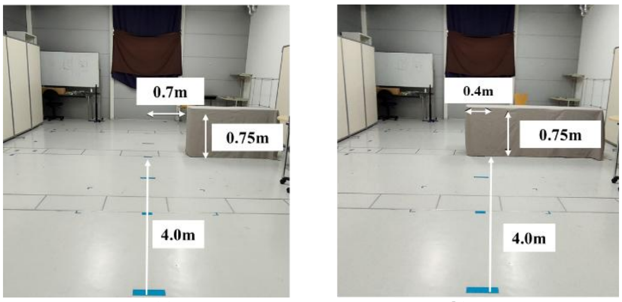

(a) (b)

Fig. 11. Walking environment. (a) Case 1: Obstacle is near the front of the path (b) Case 2: Obstacle completely blocks the path.

D. Subjects

Two normally sighted male subjects in their twenties, Sub.D and Sub.E, participated in this experiment. They performed each experiment once while blindfolded and wearing the navigation system. They were informed beforehand that there might be obstacles in their path.

The experiment was also approved by the ethics committee of Tohoku Gakuin University.

E. Results

Fig. 12 shows the results of the walking navigation performed in the Case 1 and Case 2 environments, respectively. The black boxes represent obstacles, and the red circles indicate the switching positions of the head movement based on the depth camera information. Fig. 13 illustrates the direction of the walkable area detected by the depth camera, $\theta_{pass,}$ (green line) and the orientation of the head, θ, and trunk, $\emptyset$, (black line and red dashed line).

In both cases, the head rotation control was performed twice. In Case 1, the target angle of the head, θ_d,was 30 degrees both times; in Case 2, it was 45 deg. (green dashed line).

Fig. 12 shows successful obstacle avoidance in both cases. However, the trajectories appear to include excessive detours. Fig. 13 also shows that the trunk rotated beyond the target head angle, reaching approximately 60 deg. Two factors are thought to contribute to this problem.

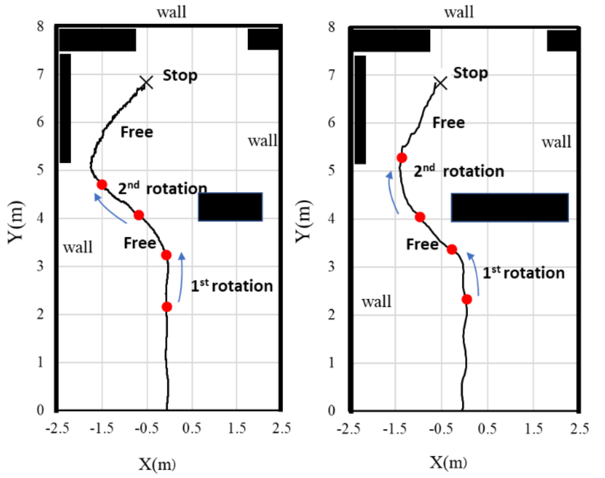

(a) Case.1 (b) Case.2

Fig. 12. Results of walking navigation for obstacle avoidance. (a) the case where there is an obstacle in front of the right side of the walking path (Sub.D), and (b) the case where the obstacle completely blocks the walking path (Sub. E).

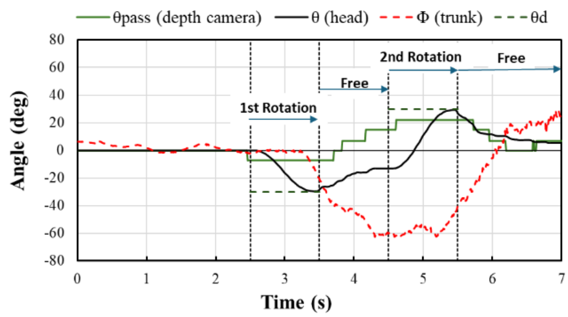

(a)

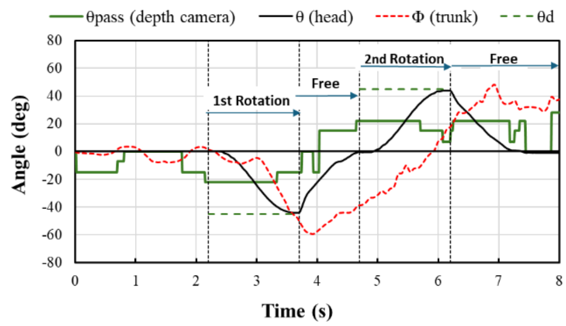

(b)

Fig. 13. Temporal Changes in Head and Trunk Orientation (a) Case 1: The trunk continues to rotate during the free-motion period after the head rotation ends, delaying the resolution of the misalignment between the two. As a result, a large rotational trajectory is generated. (b) Case 2: After the end of the head rotation, the trunk begins to follow the reverse directional motion of the head, and the misalignment between the two is resolved.

1) Excessive trunk movement due to safety concerns

Subjects were aware of the obstacle avoidance task and prioritized safety, resulting in an overreaction to head movements.

2) Delayed trunk response to free head movement

This phenomenon is particularly evident in Fig. 13(a). Even after the head reached the target angle, the trunk continued to move in the initial direction of head rotation.

This is probably due to the unstable detection of the contact force of the left and right ears, which prevented the head rotation control unit from smoothly following the free head movement (reverse rotation). It can be said that the deceleration of the trunk movement in sync with the head inversion movement was not induced. This resulted in an excessive change of direction.

To overcome this problem, we need to improve the stability of the contact force detection between the left and right ear and the device. In addition, it is crucial to optimize the head rotation speed control parameters such as threshold, f_{th} , and gain, K, in Eq. (2).

In addition, the delayed response of the trunk to head rotation (about 1.0 s) cannot be ignored. Because of this influence, it is observed that the change in walking direction does not begin until the distance to the obstacle is close to 1.0 m. Since this is unavoidable, it is necessary to activate Controlled Rotation Mode earlier by raising the obstacle detection threshold to 3.0 m or more, thus giving the user more room to avoid the obstacle.

Although some challenges were found, these experimental results show that walking navigation, including obstacle avoidance, is feasible by combining head rotation and free movement.

VI. Discussion

A. Performances: Reaction Time and Certainly

Most navigation systems convert spatial information into some form of sensory stimulus and communicate it to the user. The user must quickly and accurately understand the navigation content from these stimuli and take actions.

Many methods using vibration stimuli have been proposed, but due to the limited variety of vibration patterns, the amount of information that can be conveyed through stimulation at a single location is restricted.

On the other hand, more information can be translated by combining stimulus patterns and locations, although there is concern that this may increase presentation time and decrease perceptual accuracy.

Wave-like vibration patterns, in which multiple motors vibrate sequentially, have been studied, but their performance has been reported to be inferior to that of static stimuli in both the foot [12] and waist [14].

A system has been developed that uses seven vibration stimulation points on the forehead to convey nine walking instructions through three-point stimulation [13]. However, this system requires approximately 2,000 ms for stimulus pattern presentation and about 1,000 ms for pattern recognition, with an identification accuracy of 85%.

Another system uses a cuff-like stimulation device worn on the upper arm to induce skin shear deformations that indicate forward, stop, and left/right turns [11]. While this system provides fast response times (average 870–1,600 ms, depending on direction) but can transmit fewer instructions.

The proposed method demonstrates an advantage with an average trunk response time to head rotation of approximately 700–1,200 ms (varying between subjects). In addition, it has been confirmed that walking direction changes reliably in response to head angle, indicating the potential for fine directional control. In addition, it is a user-friendly method that only tracks system-initiated head movements and does not require cognitive processing.

User-friendly methods that do not require cognitive processing include guide dog and walker-type devices [15–17], but their size limits the situations in which they can be used.

A wearable walking navigation system using the body’s rotational response to pressure and shear deformation stimuli on the skin, called the hanger reflex, has been proposed [29]. The research reported that the hanger reflex to the head induces its rotational movements but has little effect on walking direction. The reason for this is thought to be that the moment of inertia of the head itself was small, and the acceleration was also small, so that trunk movements were not induced. On the other hand, when the waist reflex was used, the trunk rotation was directly induced and changes in walking direction were observed.

However, there is a concern that the reflex may be less reliable because it depends on the individual’s sensitivity. In addition, its application to consecutive direction change under the assumption of path guidance and obstacle avoidance is an issue to be addressed in the future.

As with the hanger reflex method, it was confirmed that the induction of trunk motion in the proposed method is uncertain for small head rotations of about 10 degrees. This may be due to the small rotational acceleration.

However, the proposed method has the potential to design head rotation patterns that reliably induce trunk responses.

Furthermore, we have shown that repeated combinations of head rotation and free movement can provide effective guidance for tasks such as obstacle avoidance, which are often required in real-world scenarios. To achieve safe and effective guidance, both the setting of the target direction and the timing of the initiation of free head movements must be carefully designed.

B. Improving Navigation Accuracy

We have found that current head rotation control methods have difficulty ensuring a perfect match between the target head angle and the final walking direction. Currently, walking direction is stabilized by allowing free head movement after reaching the target angle. This reverse head movement slows down the trunk rotation, and the walking direction is fixed when the directional mismatch between the head and trunk is resolved.

However, this method may not achieve the initial target direction due to the compensatory head movement. On the other hand, if the reverse head rotation could not be smooth or delayed, the trunk rotation exceeds the target direction. To improve the accuracy of walking navigation, it will be effective to determine the timing of initiating free head movement based on the trunk direction.

This approach requires monitoring the trunk direction using an Inertial Measurement Unit (IMU) integrated with the depth camera. In addition, analysis of the relative motion between the head and trunk will be critical in determining the optimal timing for initiating free head motion.

C. Optimal Navigation Direction

The obstacle avoidance navigation results show that the walking trajectory avoided the obstacle more than necessary. This could be due to the excessive rotation of the trunk mentioned above, but the main cause was that the target direction was not appropriate.

In these experiments, the center of the largest detected free space was used as the passing target, and the target direction was approximated by two values, 30 and 45 degrees, which had the effect of improving the safety of avoidance.

To achieve more efficient obstacle avoidance, it is necessary to make the minimum direction change necessary for avoidance. One possible solution is to divide the walkable area into areas wide enough for a person to pass, and use the area closest to the obstacle as the target direction. Another possibility is to detect more distant obstacles as avoidance targets and initiate avoidance navigation. In this case, the obstacle can be avoided efficiently with fewer direction changes. However, it would be necessary to develop a rotation pattern that would induce trunk motion even with a small head rotation angle.

D. Limitation

Frequent head rotation can overstimulate the semicircular canals and cause loss of balance. This can prevent normal trunk responses. It is therefore necessary to insert a short pause after turning the head. However, such measures are of concern because they reduce the feasibility of navigation in crowded environments and avoiding suddenly appearing obstacles.

In addition, the results of this experiment were obtained with sighted individuals, and the effects and challenges for visually impaired individuals need to be verified in the future.

VII. Conclusion

In this paper, we proposed a new navigation system for visually impaired people using trunk movements induced by head rotation.

Through several experiments, we analyzed the response of the trunk to head movements and confirmed the feasibility of this method for walking navigation. We also proposed a head control method that incorporates free head movements to achieve stable walking, and confirmed its applicability to real tasks through obstacle avoidance experiments. The user only needs to follow the head rotation controlled by the system, and does not need any cognitive processing to perceive space. This is an advantage that has not been available in conventional navigation using sensory feedback.

However, this is a first step in development, and the experiment was conducted under very simple conditions. In order to accommodate more people and different situations, it is necessary to improve the navigation performance and safety. Therefore, we would like to analyze the linkage between head and trunk movements in more detail and improve the control method for head rotation. It is also necessary to improve the ability to sense the environment.

From a safety perspective, it is necessary to consider how to handle the case where voluntary head movements and forced head rotations by the system occur simultaneously.

In the future, in addition to the local guidance considered in this study, we would like to expand the functions of the system to support independent movement and social participation of visually impaired people, such as route guidance using map information.

Conflict of Interest

The authors declare no conflict of interest.

Author Contributions

Satoshi Koharada designed and fabricated the system and conducted the experiments for evaluating the performance. Shinya Kajikawa supervised the research and wrote the paper, all authors had approved the final version.

Funding

This work was supported by JSPS KAKENHI Grant Number 22K12945.

References

[1] Projected Change in Vision Loss 2020 to 2050. The International Agency for the Prevention of Blindness (IAPB). [Online]. Available: https://www.iapb.org/learn/vision-atlas/

[2] M. M. Islam, M. S. Sadi, and T.Braunl, "Automated walking guide to enhance the mobility of visually impaired people," *IEEE Transactions on Medical, Robotics and Bionics*, vol. 2, no. 3, pp.483–496, 2020.

[3] S. Xu, C. Yang, W. Ge, C. Yu, and Y. Shi, "Virtual paving: Rendering a smooth path for people with visual impairment through vibrotactile and audio feedback," in *Proc. ACM on Interactive, Mobile, Wearable and Ubiquitous Technologies*, 2020, vo. 4, no. 3.

[4] D. Kleinberg, R. Yozevitch, I. Abekasis, Y. Israel, and E. Holdendreber, "A haptic feedback system for spatial orientation in the visually impaired: A comprehensive approach," *IEEE Sensors Letters*, vol. 7, no. 9, 2023.

[5] Y. Wang and K. J. Kuchenbecker, "HALO: Haptic alerts for low hanging obstacles in white cane navigation," in *Proc. IEEE Haptics Symposium (HAP TICS2012)*, Vancouver, 2012, pp. 527–532.

[6] S. Gallo, D. Chapuis, L. Santos-Carreras, Y. Kim *et al.*, "Augmented white cane with mulutimodal haptic feedback," in *Proc. IEEE RAS & EMB International Conference on Biomedical Robotics and Biomechatoronics (EMBS2010)*, Tokyo, 2010, pp.149–155.

[7] R. Pyun, Y. Kim, P. W. Roger, and S. Schneller, "Advanced augmented white cane with obstacle height and distance feedback," in *Proc. IEEE International Conference on Rehabilitation Robotics (ICORR2013)*, Seattle, 2013.

[8] C. Stoll, R. Palluel-Germain, V. Fristot, D. Pellerin, D. Alleysson, and C. Graff, "Navigating from a depth image converted into sound," *Applied Bionics and Biomechanics*, vol. 2015, 543492, 2015.

[9] Y. H. Lee, and G. G. Medioni, "RGB-D camera based wearable navigation system for the visually impaired," *Computer Vision and Image Understanding*, 149, pp. 3–20, 2016.

[10] H. C. Wang,R. K. Katzschmann,S. Teng, B. Araki, L. Giarre, and D. Rus,"Enabling indenendent navigation for visually impaired people through a wearable vision-based feedback system", in *Proc.*

IEEE International Conference on Robotics and Automation (ICRA2017), Singapore, 2017, pp.6533–6540.

[11] F. Barontini, M. G. Catalano, L. Pallottino, B. Leporini, and M. Bianchi, "Integrating wearable haptics and obstacle avoidance for the visually impaired in indoor navigation: A user-centered approach," *IEEE Transactions on Haptics*, vol. 14, no. 1, pp.109–122, 2021

[12] A. Cosgun, E. A. Sisbot, and H. I. Christensen,"Guidance for human navigation using a vibro-tactile belt interface and robot-like motion planning," in *Proc. IEEE International Conference on Robotics and Automation*, 2014, pp.6351–6355.

[13] S. Ma, P. X. Liu, and J. Gao, "A novel head-mounted navigation device based on vibrotactile stimulation," *IEEE Transactions on Instrumentation and Measurement*, vol. 73, 2024.

[14] R. Velazquez, O. Bzazan, C. Alonso, and C. Delgado-Mata, "Vibrating insoles for tactile communication with the feet," in *Proc. IEEE International Conference on Advanced Robotics*, 2011, pp. 118–123.

[15] A. J. Kolarik, R. Raman, B. C. Moore, S. Cirstea, S. Gopalakrishnan, and S. Pardhan, "The accuracy of auditory spatial judgments in the visually impaired is dependent on sound source distance," *Scientific Reports*, vol. 10, 7169, 2020.

[16] I. Ulrich and J. Borenstein, "The guide cane—Applying mobile robot technologies to assist the visually impaired," *IEEE Trans. on Systems*, Man, *and Cybernetics—Part A: Systems and Humans*, vol. 31, no. 2, pp. 131–136, 2001.

[17] Y. Wei, X. Kou, and M. C. Lee, "A new and navigation research for a guide-dog robot system in urban system", in *Proc. IEEE International Conference on Advanced Intelligent Mechatronics*, 2014, pp. 1290–1295.

[18] J. Guerreiro, D. Sato, S. Asakawa, H. Dong, K. M. Kitani, and C. Asakawa, "CaBot: Designing and evaluating an autonomous navigation robot for blind people," in *Proc. the 21st International ACM SIGACCESS Conference on Computers and Accessibility*, 2019, pp. 68–82.

[19] S. Kajikawa, I. Watanabe, and H. Hoshi, "Physical interaction based traveling aid system with depth camera and unevenness detection mechanism," *International Journal of Mechanical Engineering and Robotics Research*, vol. 11, no. 10, pp. 767–776, 2022.

[20] A. M. Lopez, J. C. Alvarez, and D. Alvarez, "Walking turn prediction form upper body kinematics: A systematic review with implications for human-robot interaction," *Applied Sciences*, vol. 9, 361, 2019.

[21] M. A. Hollands, K. L. Sorenson, and A. E. Patla, "Effects of head immobilization on the coordination and control of head and body reorientation and translation during steering," *Experimental Brain Research*, vol. 140, pp. 223–233, 2001.

[22] L. A. Vallis, A. E. Patla, and A. L. Adkin, "Age-related modifications in steering behavior: effects of base-of-support constraints at the turn point," *Experimental Brain Research*, vol. 190, pp. 1–9, 2008.

[23] D. Bernardin, H. Kadone, D. Bennequin, T. Sugar, M. Zaoui, and A. Berthoz, "Gaze anticipation during human locomotion," *Experimental Brain Research*, vo. 223, pp. 65–78, 2012.

[24] R. Grasso, P. Prevost, Y. P. Lvanenko, and A. Berthoz, "Eye-head coordination for the steering of locomotion in humans: An anticipatory synergy," *Neuroscience Letters*, vol. 253, pp. 115–118. 1998.

[25] L. A. Vallis and A. E. Patla, and A. L. Adkin, "Control of steering in the presence of unexpected head yaw movements", *Experimental Brain Research*, vol. 138, pp. 128–134, 2001.

[26] L. A. Vallis and A. E. Patla, "Expected and unexpected head yaw movements result in different modifications of gait and whole body coordination strategies," *Experimental Brain Research*, vol. 157, pp. 94–110, 2004.

[27] T. Pozzo, B. A. Lefort, "Head stabilization during various locomotor tasks in humans," *Experimental Brain Research*, vol. 82, no. 1, pp. 97–106, 1990.

[28] M. Pfeiffer, T. Dunte, S. Schneegass, F. Alt, and M. Rohs,"Cruise control for pedestrians: Controlling walking direction using electrical muscle stimulation," in *Proc. the 33rd Annual ACM Conference on Human Factors in Computing Systems*, pp. 2505–2514, 2015.

[29] T. Maeda, H. Ando, T. Amemiya, M. Inami, N. Nagaya, and M. Sugimoto, "Shaking the world—Galvanic vestibular stimulation as a novel sensation interface," *ACM SIGGRAPH Emerging Technologies*, 2005.

[30] Y. Kon, T. Nakamura, M. Sato, and H. Kajimoto, "Effect of hanger reflex on walking," in *Proc. IEEE Haptics Symposium*, 2016, pp. 313–318.

[31] T. Flash and N. Hogan, "The coordination of arm movements: An experimentally confirmed mathematical model," *The Journal of Neuroscience,* vol. 5, no. 7, pp. 1688–1703, 1985.